2005 SCEC Report

INFERENCE OF CRUSTAL RHEOLOGY FROM OBSERVATIONS OF POSTSEISMIC DEFORMATION FOLLOWING THE 2004 PARKFIELD, CALIFORNIA EARTHQUAKE

Principal Investigators:

Andrew M. Freed
Earth & Atmospheric Sciences
Purdue University
550 Stadium Mall Drive
West Lafayette, IN 47907
Phone: (765)496-3738
Fax: (765) 496-1210
freed@purdue.edu

Roland Bürgmann
Earth & Planetary Sciences
University of California
389 McCone Hall
Berkeley, CA 94720
Phone (510) 643-9545
Fax (510) 643-9980
burgmann@seismo.berkeley.edu

Introduction

Well monitored earthquakes can be used as rock deformation experiments from which to infer the mechanisms and strength that govern the lithosphere's response to loading. The December 22, 2003 San Simeon - September 28, 2004 M6 Parkfield, California earthquake sequence presents a unique opportunity to infer rheologic properties in the Southern California crust, especially in the vicinity of the Earthscope SAFOD site. Never before has postseismic deformation associated with a relatively small event been so well observed by a network of continuous GPS measurements and InSAR acquisitions. By using a finite element model that considers both earthquakes, we will test hypotheses regarding the relative importance of various candidate postseismic mechanisms (including viscous relaxation, afterslip, and poroelastic rebound).

The beauty of having the opportunity to study postseismic deformation associated with a well monitored small event such as Parkfield is that the energy imparted is likely only sufficient to induce a postseismic response in the crust (Figure 1). Without the added complexity of mantle processes, the Parkfield earthquake can be used as a rock deformation experiment isolating the crustal response. This should enable us to more directly test several important hypotheses: (1) afterslip occurs in the shallow crust in areas of coseismic slip deficit and velocity strengthening fault rheology, (2) the lower crust is relatively strong, (3) deformation in the lower crust is controlled by power-law flow, and (4) poroelastic rebound is a significant postseismic process.

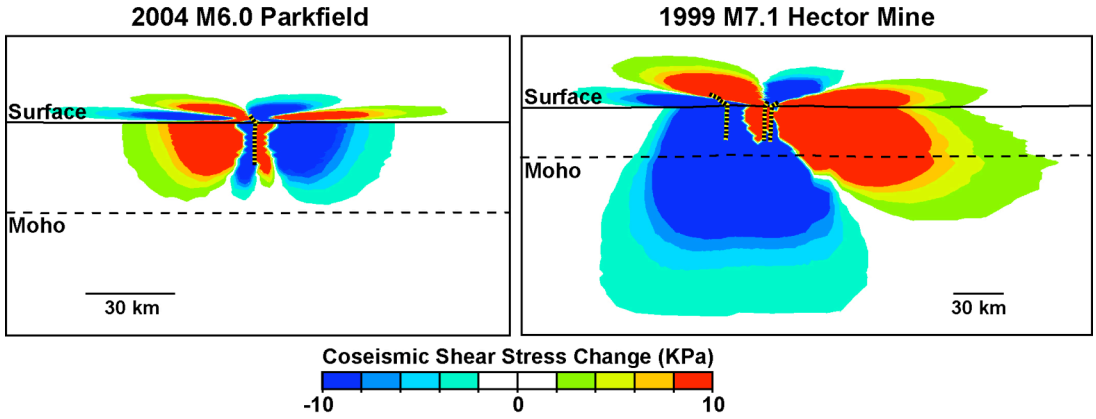

Figure 1. Comparison of coseismic shear stress changes induced by the Parkfield and Hector Mine earthquakes. Shown is a cross section through the respective faults from our finite element models.

Results

In the first phase of our project, we have focused on compiling and analyzing deformation data spanning both the San Simeon (Rolandone et al., 2005, manuscript in preparation for submission to Geophys. Res. Lett.) and Parkfield earthquakes (Johanson et al., 2005, manuscript submitted to Bull. Seismol. Soc. Am., Johnson et al., 2005, manuscript submitted to Bull. Seismol. Soc. Am.) and their postseismic episodes. We developed kinematic models of these events, focusing on kinematic slip models and mechanical models of afterslip that clearly dominates the early postseismic period following the Parkfield earthquake.

We inverted InSAR data jointly with campaign and continuous GPS data for slip in the coseismic and postseismic periods of the 2004 Parkfield earthquake. The InSAR dataset consists of eight interferograms from data collected by the Envisat and Radarsat satellites spanning the time of the earthquake and variable amounts of the postseismic period. Thus, model inversions have to separate deformation from the coseismic event and the afterslip. Figure 2 shows the observed range change patterns and respective contributions of coseismic and postseismic models to the total deformation. The model assumes exponential decay of the postseismic slip with a decay time constant of 0.17 years, determined from time series analysis of continuous GPS and creepmeter data. The model analysis utilizes the SAR interferograms, as well as all continuous (SCIGN/BARD/U. Wisconsin) and campaign GPS data (UCB, USGS) we have obtained to date.

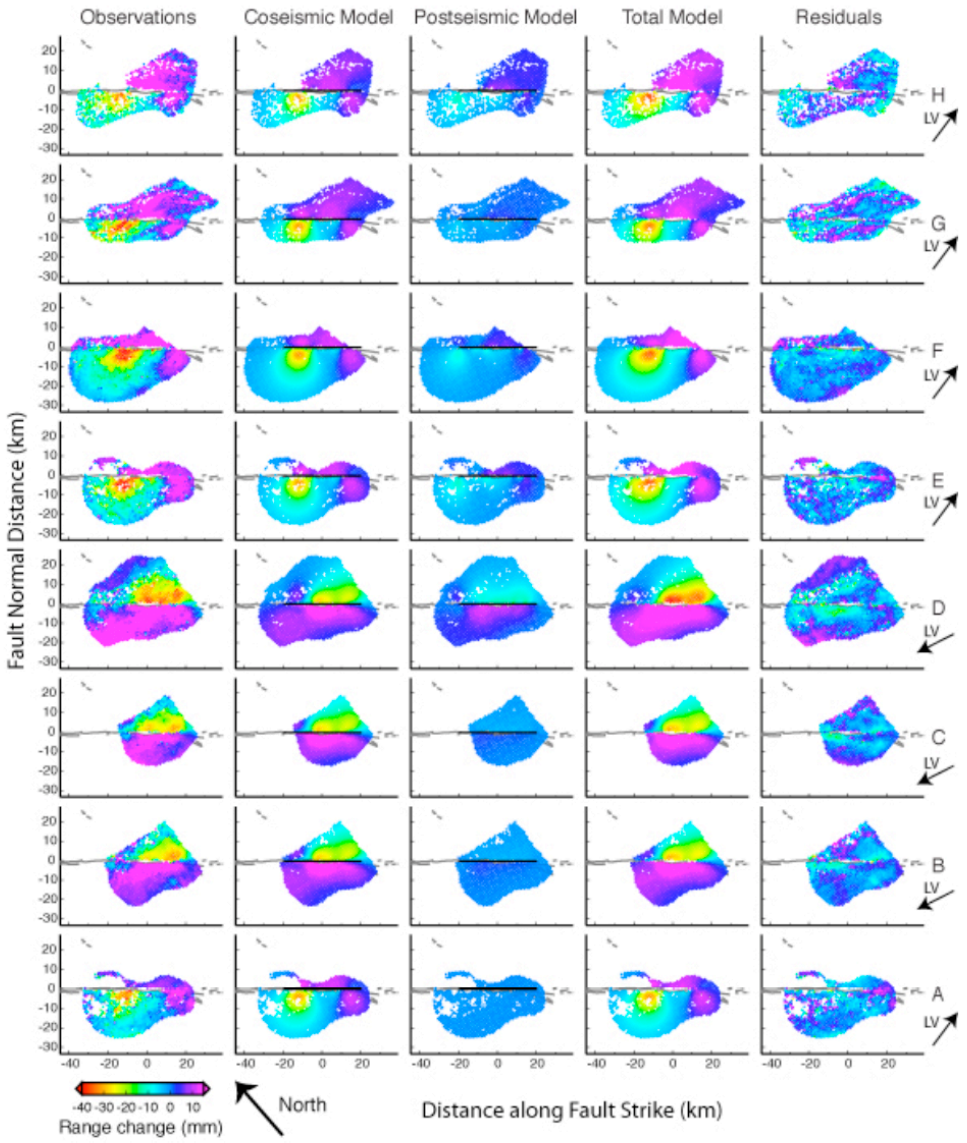

Figure 2. Model fits to eight ENVISAT and RADARSAT interferograms spanning the Parkfield earthquake and various amounts of postseismic deformation. LV: Look vector, direction of satellite view.

Figure 3 shows the estimated coseismic slip distribution and postseismic afterslip patterns based on this analysis (Johanson et al., 2005, submitted to Bull. Seismol. Soc. Am.). We find a geodetic moment magnitude of Mw 6.2 for the coseismic rupture and Mw 6.1 for the entire postseismic period. The coseismic rupture occurred mainly in two slip asperities; one near the hypocenter and the other 15-20 km north. Shallow postseismic slip occurred mainly on the fault areas surrounding the coseismic rupture, including the rupture areas of two Mw5.0 aftershocks. A comparison of the geodetic slip models with seismic moment estimates suggests that the postseismic moment release of the Parkfield earthquake is as much as 70% of the total. This underlines the importance of aseismic slip in the slip budget for the Parkfield segment. Comparison of these models with those obtained by considering even shorter periods (high-

frequency GPS, creep and strain data) suggests that some of the slip mapped on the coseismic rupture actually occurred during the first day(s) of the postseismic period (Johnson et al., 2005 and Langbein et al., 2005, submitted to Bull. Seismol. Soc. Am.)

.

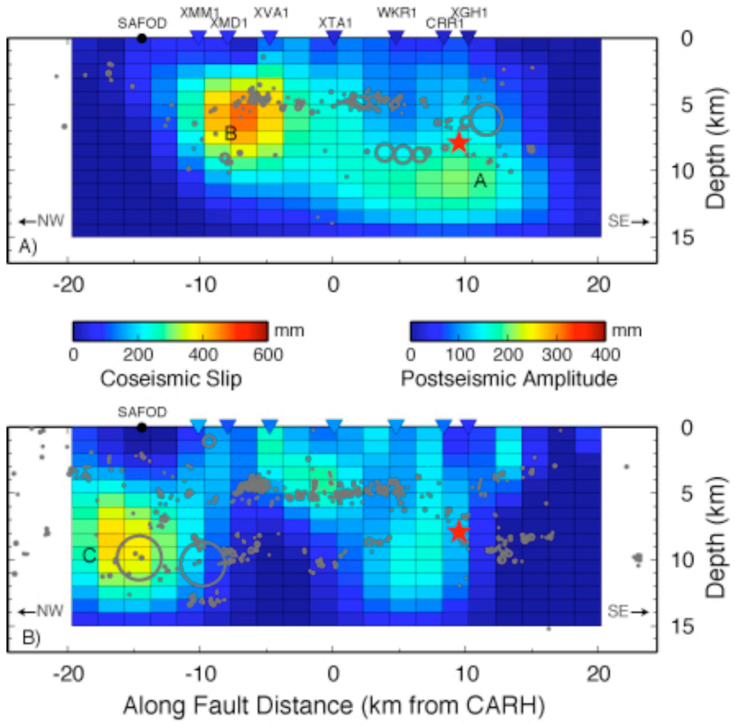

Figure 3. Results of inversion for a) Coseismic slip b) Amplitude of postseismic exponential. Red stars mark location of earthquake hypocenter. Gray circles are double-difference relocated aftershocks [Thurber et al., Submitted], size of circle is size of rupture assuming 3 MPa stress drop and circular rupture. Letters A, B & C refer to asperities mentioned In the text. Triangles are color-coded creepmeter displacements.

Ongoing Work and Discussion

In the next phase of this project, we will analyze data spanning later portions of the postseismic transient deformation, to evaluate evidence for a contribution of viscous flow and poroelastic rebound to the observed deformation field. Figure 4 shows synthetic interferograms with the predicted range change pattern from viscous relaxation in the lower crust or upper mantle, as well as from adjustment of fluid pressures (poroelastic rebound). Note that range change associated with postseismic relaxation is consistent with observation of highest range increase (subsidence) to the west of the northern part of the surface rupture. As this is similar to the coseismic and afterslip induced changes, it will be a challenge to separate these signals. In addition, we must consider that postseismic relaxation may not only be initiated by coseismic stress changes, but also by significant early afterslip. Now that we are a year past the earthquake, our first step will be to see if the pattern of postseismic deformation has changed, potentially indicating a change in mechanism. Such a recognition will be important to separate out postseismic mechanisms. This is the thrust of our current effort.

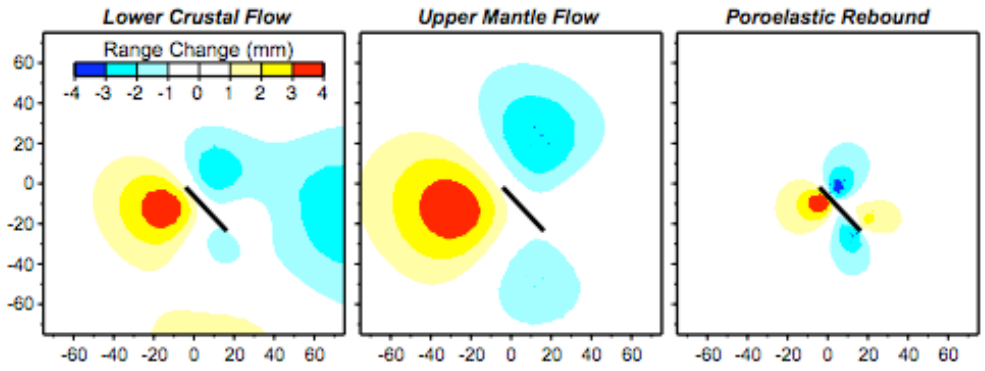

Figure 4. Predicted range-change pattern (assuming ERS descending orbit data) from viscous relaxation in the lower crust (left), viscous flow in the upper mantle (middle), and poroelastic rebound (right). Models assume complete relaxation of coseismic stress changes.

The 2004 Parkfield earthquake is particularly interesting for two reasons. First, it occurred about two decades after its expected date based on the average recurrence interval of the past six events on this segment. And second, the Parkfield segment is next to the Cholame section of the San Andreas fault, where the 1857 M=7.9 Fort Tejon earthquake initiated and may be late in its earthquake cycle. It is also reasonable to consider that the San Simeon earthquake loaded the Parkfield segment, leading to its triggering less then a year later, and that the Parkfield earthquake has loaded and will continue to load the Cholame segment. We will infer how stresses are evolving due to postseismic mechanisms once we begin to understand the nature of the postseismic response. Figure 5 shows a preliminary calculation of shear stress change imparted on the Cholame segment by the Parkfield earthquake may look like due to coseismic slip and a year of lower crustal flow. All indications are that the northern edge of the Cholame segment has been brought closer to failure and this loading will likely continue for some time. This inference will be tested by our continuing effort to understand postseismic processes.

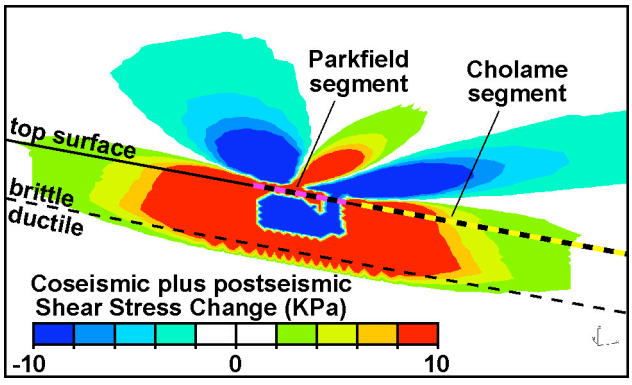

Figure 5. Preliminary calculated shear stress changes imparted on the northern edge of the Cholame segment of the San Andreas fault by the Parkfield earthquake and hypothetical lower crustal flow. View is from a cross section of a finite element model along the San Andreas fault.

References

Johansen, I. A., E. J. Fielding, F. Rolandone, and R. Bürgmann (2006), Coseismic and postseismic slip of the 2004 Parkfield earthquake from space-geodetic data, *Bull. Seism. Soc. Am.*, *submitted 09/15/05*.

Johnson, K. M., R. Bürgmann, and K. M. Larson (2006), Frictional afterslip following the 2004 Parkfield, California earthquake, *Bull. Seism. Soc. Am.*, *submitted 09/15/05.*

Rolandone, F., D. S. Dreger, M. H. Murray, and R. Bürgmann (2005), Coseismic Slip Distribution of the 2003 Mw 6.5 San Simeon earthquake, California, determined from GPS measurements and seismic waveform data, *Geophys. Res. Lett.*, *in prep*.